

THE SECOND DATA RELEASE OF THE KODIAQ SURVEY

J.M. O'MEARA¹, N. LEHNER², J.C. HOWK², J.X. PROCHASKA³, A.J. FOX⁴, M.S. PEEPLES^{4,5}, J. TUMLINSON^{4,5}, B.W. O'SHEA⁶

Submitted to the Astronomical Journal

ABSTRACT

We present and make publicly available the second data release (DR2) of the Keck Observatory Database of Ionized Absorption toward Quasars (KODIAQ) survey. KODIAQ DR2 consists of a fully-reduced sample of 300 quasars at $0.07 < z_{\text{em}} < 5.29$ observed with HIRES at high resolution ($36,000 \leq R \leq 103,000$). DR2 contains 831 spectra available in continuum normalized form, representing a sum total exposure time of ~ 4.9 megaseconds on source. These co-added spectra arise from a total of 1577 individual exposures of quasars taken from the Keck Observatory Archive (KOA) in raw form and uniformly processed. DR2 extends DR1 by adding 130 new quasars to the sample, including additional observations of QSOs in DR1. All new data in DR2 were obtained with the single-chip Tektronix TK2048 CCD configuration of HIRES in operation between 1995 and 2004. DR2 is publicly available to the community, housed as a higher level science product at the KOA and in the *igm spec* database (v03).

Keywords: absorption lines – intergalactic medium – Lyman limit systems – damped Lyman alpha systems

1. INTRODUCTION

The High-Resolution Echelle Spectrograph (Vogt et al. 1994, HIRES) on the Keck I telescope has been a spectacular instrument for the study of intergalactic and circumgalactic gas around galaxies since its introduction in 1994. The large aperture of Keck I coupled with the high spectral resolution of HIRES ($R \approx 35,000 - 100,000$) gave rise to a 20 year golden age of QSO absorption line studies. HIRES has allowed the best determinations of the primordial D/H ratio (Burles & Tytler 1998; O'Meara et al. 2001; Cooke et al. 2014), a test of Big Bang nucleosynthesis and fundamental physics, and it provided high precision constraints on the fine-structure constant (Murphy et al. 2001, 2003). HIRES has been instrumental in studying the physics of the intergalactic medium (IGM) and thereby cosmology (Rauch et al. 1997; Simcoe et al. 2004; Tytler et al. 2009; Bolton et al. 2014), including the highest redshifts accessible at the end of reionization (Bolton et al. 2010; Becker et al. 2011). HIRES has played leading roles in the determination of the metallicity distribution in and physics of damped Ly α systems (Wolfe et al. 2005; Rafelski et al. 2012). HIRES has also been critical in the study of circumgalactic gas at all redshifts (Rudie et al. 2012; Lehner et al. 2013; Werk et al. 2013; Wotta et al. 2016), including in setting the scale for the Milky Way's high velocity cloud population (Thom et al. 2008; Wakker et al. 2007,

2008; Smoker et al. 2011).

As part of their contribution to the Keck Observatory, NASA has provided an archival service to give access to the data from HIRES (and now the other Keck instruments as well). The Keck Observatory Archive (KOA)⁷ holds the vast majority of all HIRES observations of distant QSOs. These data are publicly accessible to all interested researchers. However, they are nominally only available in their raw form. Given the idiosyncrasies of data collection by a large number of observers operating under disparate conditions, there is a significant hurdle to using these data directly for science. This is especially true given the difficulties in coaddition, a process requiring an order-by-order continuum placement for optimal results.

In order to address these issues, we have undertaken a NASA-funded processing of all of the extant HIRES data for the study of QSO absorption lines to provide fully-reduced QSO spectra to the community. This first data release (DR1) of our Keck Observatory Database of Ionized Absorption toward Quasars (KODIAQ) was presented in O'Meara et al. (2015), which included spectra for 170 QSOs. The original science goal of the KODIAQ survey has been to study of the O VI absorption in strong HI absorbers at high $z > 2.2$ (Lehner et al. 2014), revealing unique properties of these absorbers. Besides our original program the data making up DR1 have motivated our new KODIAQ Z survey aimed to determine the metallicity of the strong HI absorbers ($15 < \log N_{\text{HI}} < 19$) at $z > 2$, and have been used in a number of new surveys. These include the characterization and interpretation of the small-scale structure in the Ly α forest (Rorai et al. 2017), the metallicity distribution of of strong H I systems at intermediate- and high-redshifts (Fumagalli et al. 2016; Lehner et al. 2013, 2016; Wotta et al. 2016), the statistical characterization of Mg II and LLS absorbers

¹ Department of Chemistry and Physics, Saint Michael's College, One Winooski Park, Colchester, VT 05439

² Department of Physics, University of Notre Dame, 225 Nieuwland Science Hall, Notre Dame, IN 46556

³ University of California/Lick Observatory, Santa Cruz, 1156 High Street, CA 95064

⁴ Space Telescope Science Institute, 3700 San Martin Drive, Baltimore, MD, 21218

⁵ Department of Physics and Astronomy, Johns Hopkins University, Baltimore, MD 21218

⁶ Department of Computational Mathematics, Science and Engineering, Michigan State University, East Lansing, MI 48824

⁷ <http://www2.keck.hawaii.edu/koa/public/koa.php>

(Mathes et al. 2017; Prochaska et al. 2015), characterization of extremely low metallicity gas, including for the determination of primordial D/H (Cooke et al. 2016; Crighton et al. 2016), and even the study of the extended reaches of extremely low-redshift galaxies (Dutta et al. 2016).

The DR1 datasets were confined to those taken after the HIRES upgrade to a three-CCD mosaic in 2004 due to the shift in data reduction approach associated with that upgrade. This excluded the first decade of HIRES data, including many exceptional datasets. Here we present KODIAQ DR2, which now includes HIRES spectra of QSOs from the years 1995–2004. Our paper lays out our data reduction approach, which varies somewhat from that discussed in O'Meara et al. (2015) due to the difference in detectors, and presents the statistics of the combined DR1+DR2 datasets. Together these releases contain 300 QSOs covering the redshift range $0.07 \lesssim z_{\text{em}} \lesssim 5.29$. All of the data presented here are now available through the KOA and will be available with the distribution of v03 of the `specdb` dataset⁸ (Prochaska 2017).

2. THE DATA

A full discussion of HIRES and its data, including the process of downloading and ingesting the raw data into the KODIAQ database is presented in O'Meara et al. (2015). The new data presented here in DR2 all stem from HIRES observations by multiple PIs between 1995 and 2004. Table 1 presents the HIRES deckers used across DR2 and their corresponding spectral resolution. As with DR1, the majority of observations were made with the C1 or C5 decker providing ≈ 6 and $\approx 8 \text{ km s}^{-1}$ FWHM resolution respectively.

Data obtained prior to the HIRES upgrade in 2004 had slightly reduced total spectral coverage due to the size of the detector. As a result, observations were frequently made in matched sets where the echelle angle was kept fixed, but the cross-disperser angle varied so as to provide fewer spectral gaps, particularly at redder wavelengths. The overall throughput of the pre-2004 detector was lower, resulting in a longer average per-exposure integration time as compared to post-2004 upgrade observations.

2.1. Data Reduction

The data reduction largely followed the same procedures as outlined in O'Meara et al. (2015). However, for the new data in DR2, only data in the single-chip configuration was reduced, whereas in O'Meara et al. (2015), only three-chip mosaic data was involved. Minor differences in the data reduction with HIRedux data reduction package⁹ arise from the change in detectors. First, the single-chip detector has a blemish known as the “ink spot” in the center of the detector. The pixels associated with the ink spot were masked in the extracted spectrum and ignored in any further processing so as not to confuse it with real QSO absorption lines. Second, the flat fielding procedure from O'Meara et al. (2015) was not applied as the instrument was changed in 2004, thus

negating the ability to construct the nominal HIRedux pixel flats. Instead, we use the internal flats both for order edge identification and pixel flat-fielding.

Finally, multiple spectra showed significant echelle order overlaps in their bluest orders. Typically at wavelengths $\lambda < 3800\text{\AA}$, significantly complicating sky subtraction, source identification, and source extraction. In most cases, these orders were trimmed off. Therefore, the spectral coverage of these objects is smaller than is quoted in the KOA. It is also worth noting that the pre-2004 hires detector was far less blue sensitive than its successor. As a result, observations at very blue ($\lambda < \sim 3400\text{\AA}$) wavelengths often had very long exposure times, some in excess of two hours per integration. For these exposures, unless a number of other exposures of the same object were taken with the same setup, cosmic ray rejection will likely not be optimal. As with the DR1, continua were fit on an order-by-order basis in the manner described in O'Meara et al. (2015). The full DR2 sample contains over 15000 echelle orders that have been continuum fit.

2.2. KODIAQ at the KOA and `igmspec`

As with DR1, the DR2 data products are available for community download from the KOA. DR2 supersedes DR1 at the KOA and contains the full 300 quasar sample. As with DR1, users may search for and download individual DR2 quasar sight line flux and error spectra, or the full DR2 sample all at once. Machine readable tables and files exist for each spectrum to link back to the raw KOA data as needed. DR2 also makes available all intermediate data reduction steps grouped on an observing run by observing run basis. Spectra from DR2 are also available in the v03 release of the `igmspec` database (see Prochaska (2017) for details).

3. PROPERTIES OF KODIAQ DR2

The KODIAQ DR2 comprises HIRES observations of 300 quasar lines of sight in total. Of these, 130 quasar sight lines are new since DR1, along with many new additional observations of some of the DR1 quasars. Table 2 presents the new data since DR1. As in O'Meara et al. (2015), quasars are named according to their J2000 R.A./Decl. coordinates as resolved by either SIMBAD or SDSS. Many quasars were observed by multiple PIs in multiple instrument configurations. For a given PI+configuration, the data were combined. Table 2 lists the exposure time of the combined spectra, including the wavelength coverage of the spectra after trimming poorly extracted orders when necessary (see above). We note that these exposure times are only a crude measure of data quality, as they do not include the observing conditions.

Table 3 presents the full DR2 sample of 300 quasars. The rest wavelengths listed in Table 3 are given at the quasar emission redshift, i.e. $\lambda_r = \lambda_{\text{obs}} / (1.0 + z_{\text{em}})$. The full DR2 comprises 1577 individual exposures, grouped into 831 spectral co-adds. The aggregate exposure time of the full DR2 sample is ~ 4.9 megaseconds. DR2 represents a significant increase over DR1, which was comprised of 170 quasar sight lines, 240 co-additions, 567 individual exposures, and 1.6 megaseconds of total exposure time.

⁸ <http://github.com/specdb>

⁹ <http://www.ucolick.org/~xavier/HIRedux/>

3.1. General Properties

Figure 1 shows the quasar redshift distribution for the DR2 sample, including the distribution for the 130 new quasars alone. DR2 spans a range in redshift from $0.07 < z_{\text{em}} < 5.29$, with a median redshift of $\bar{z}_{\text{em}} = 2.586$ and a standard deviation of $\sigma_{z_{\text{em}}} = 0.918$. The distribution of DR2 quasars on the sky is shown in Figure 2. To illustrate the properties of DR2, we have performed a further co-addition of the data to produce a single spectrum per quasar. For each quasar, the co-addition re-samples the data onto a single binning and resolution. The figures in O’Meara et al. (2015) largely summarize the DR1 in a different manner, applying to the spectra co-added within a particular instrument setup.

Figure 3 displays the median S/N, as calculated by $\frac{S}{N} = \frac{1.0}{\sigma}$ per pixel of the DR2 within $\pm 5\text{\AA}$ of three rest wavelengths. The pixels are a constant 2.1 km s^{-1} for pre-2004 observations, 2.6 km s^{-1} for post-2004 observations, or 2.6 km s^{-1} for co-additions of observations mixing pre- and post-2004 data. The rest wavelengths were chosen to illustrate the viability for DR2 to be used for surveys of metal line, Ly α , and Lyman limit absorption. As can be seen in Figure 3, a significant number of quasars have high S/N, with many exceeding S/N 50 per pixel.

3.2. Cosmological Properties

The DR2 represents a significant increase over DR1 in its ability to provide a rich data sample for cosmological studies. We highlight a number of the DR2 properties below with respect to its ability to be used for surveys of metal line and HI absorption.

Figure 4 shows the rest wavelength (quasar redshift frame) spectral coverage of DR2. Well over 200 quasars in DR2 cover rest wavelengths corresponding to Ly α and C IV, and approximately 100 quasars cover the quasar Lyman limit. Figure 5 displays the redshift range over which certain ions may appear in the DR2 spectra. It bears noting that this figure is optimistic in that although certain ions (such as C IV) could appear in DR2 spectra, they may be blended with Lyman- α forest absorption from higher redshifts. Nevertheless, Figure 5 demonstrates that searches for ionic absorption in DR2 data, particularly at redshifts near $z = 2.5$ are likely to have strong statistical power.

A further illustration of this point is found in figure 6 which displays the redshift coverage of certain ions and their numbers at or above certain S/N cuts in the data. Again, Ly α and C IV stand out in terms of their numbers and data quality, but we also note that a significant number of high quality spectra exist covering Mg II absorption, albeit subject to the same caveat that some of the Mg II spectral coverage overlaps with higher redshift Lyman- α forest. Many tens of spectra have S/N in excess of 100, making DR2 the largest collection of high resolution, high signal to noise quasar spectra openly available to the community.

Finally, Figure 7 gives the redshift sensitivity function $g(z)$ for DR2. Unlike the previous figures, we consider specific wavelength ranges in the spectra to calculate $g(z)$. As in O’Meara et al. (2015), we select only the regions within a given quasar spectrum between 3000

km s^{-1} to the red of the quasar Ly β line and 3000 km s^{-1} to the blue of the quasar Ly α line for the $g(z)$ calculation of the redshift sensitivity to Ly α absorption. For C IV, we use the same 3000 km s^{-1} windows, but for the Ly α and C IV emission lines, respectively. The high frequency variations in $g(z)$ stem from the blaze function of the echelle orders, and various sharp features usually arise from detector defects or gaps in spectral coverage.

4. SUMMARY AND FUTURE

We have presented here and made public at the KOA the DR2 of the KODIAQ survey. DR2 contains spectra of 300 individual quasars obtained with HIRES since 1995. The data vary in signal to noise and resolution, but a significant subset of the DR2 is of high enough quality to facilitate a number of precision studies of the intergalactic and circumgalactic medium between $0.15 < z < 5$.

With DR2, a significant fraction of the total number of quasar observations made with HIRES since 1995 has been released to the community. We intend one final data release of HIRES data which will mix the remaining pre- and post-2004 data available from the KOA that can be nominally reduced. This final data release is anticipated in 2019–2020. As part of KODIAQ z, we will also reduce and distribute all quasars observed with the ESI instrument on Keck-II in ~ 2020 .

When using data products from DR2, in addition to the standard KOA acknowledgement (including acknowledgement to the original PIs of each program), we request that the community please include the following acknowledgement: “*Some/all the data presented in this work were obtained from the Keck Observatory Database of Ionized Absorbers toward QSOs (KODIAQ), which was funded through NASA ADAP grants NNX10AE84G and NNX16AF52G along with NSF award number 1516777*” and to cite this paper and O’Meara et al. (2015).

Support for this work was made by NASA through the Astrophysics Data Analysis Program (ADAP) grants NNX10AE84G and NNX16AF52G, along with NSF grant award number 1516777. This research has made use of the Keck Observatory Archive (KOA), which is operated by the W. M. Keck Observatory and the NASA Exoplanet Science Institute (NExSci), under contract with the National Aeronautics and Space Administration. The data presented herein were obtained at the W.M. Keck Observatory, which is operated as a scientific partnership among the California Institute of Technology, the University of California and the National Aeronautics and Space Administration. The Observatory was made possible by the generous financial support of the W.M. Keck Foundation.

The authors wish to recognize and acknowledge the very significant cultural role and reverence that the summit of Mauna Kea has always had within the indigenous Hawaiian community. We are most fortunate to have the opportunity to conduct observations from this mountain. The authors wish to recognize and sincerely appreciate the work of the entire WMKO staff over the last two-plus decades, and to the efforts of the team at the NASA Exoplanet Science Institute (NExSci) who are responsible for maintaining the KOA. Finally, we continue to dedicate this work to the late astronomers Arthur Wolfe and Wal

Sargent, and extend the dedication to the late Jerry Nelson, without whom the Keck telescopes and their great impact on science would not exist.

REFERENCES

- Becker, G. D., Sargent, W. L. W., Rauch, M., & Calverley, A. P. 2011, ApJ, 735, 93
- Bolton, J. S., Becker, G. D., Haehnelt, M. G., & Viel, M. 2014, MNRAS, 438, 2499
- Bolton, J. S., Becker, G. D., Wyithe, J. S. B., Haehnelt, M. G., & Sargent, W. L. W. 2010, MNRAS, 406, 612
- Burles, S., & Tytler, D. 1998, ApJ, 499, 699
- Cooke, R. J., Pettini, M., Jorgenson, R. A., Murphy, M. T., & Steidel, C. C. 2014, ApJ, 781, 31
- Cooke, R. J., Pettini, M., Nollett, K. M., & Jorgenson, R. 2016, ApJ, 830, 148
- Crighton, N. H. M., O'Meara, J. M., & Murphy, M. T. 2016, MNRAS, 457, L44
- Dutta, R., Gupta, N., Srianand, R., & O'Meara, J. M. 2016, MNRAS, 456, 4209
- Fumagalli, M., O'Meara, J. M., & Prochaska, J. X. 2016, MNRAS, 455, 4100
- Lehner, N., et al. 2013, ApJ, 770, 138
- Lehner, N., O'Meara, J. M., Fox, A. J., Howk, J. C., Prochaska, J. X., Burns, V., & Armstrong, A. A. 2014, ApJ, 788, 119
- Lehner, N., O'Meara, J. M., Howk, J. C., Prochaska, J. X., & Fumagalli, M. 2016, ApJ, 833, 283
- Mathes, N. L., Churchill, C. W., & Murphy, M. T. 2017, ArXiv e-prints
- Murphy, M. T., Webb, J. K., & Flambaum, V. V. 2003, MNRAS, 345, 609
- Murphy, M. T., Webb, J. K., Flambaum, V. V., Dzuba, V. A., Churchill, C. W., Prochaska, J. X., Barrow, J. D., & Wolfe, A. M. 2001, MNRAS, 327, 1208
- O'Meara, J. M., et al. 2015, AJ, 150, 111
- O'Meara, J. M., Tytler, D., Kirkman, D., Suzuki, N., Prochaska, J. X., Lubin, D., & Wolfe, A. M. 2001, ApJ, 552, 718
- Prochaska, J. X. 2017, Astronomy and Computing, 19, 27
- Prochaska, J. X., O'Meara, J. M., Fumagalli, M., Bernstein, R. A., & Burles, S. M. 2015, ApJS, 221, 2
- Rafelski, M., Wolfe, A. M., Prochaska, J. X., Neeleman, M., & Mendez, A. 2012, ApJ, 755, 89
- Rauch, M., et al. 1997, ApJ, 489, 7
- Rorai, A., et al. 2017, Science, 356, 418
- Rudie, G. C., et al. 2012, ApJ, 750, 67
- Simcoe, R. A., Sargent, W. L. W., & Rauch, M. 2004, ApJ, 606, 92
- Smoker, J. V., Fox, A. J., & Keenan, F. P. 2011, MNRAS, 415, 1105
- Steidel, C. C., Erb, D. K., Shapley, A. E., Pettini, M., Reddy, N., Bogosavljević, M., Rudie, G. C., & Rakic, O. 2010, ApJ, 717, 289
- Suzuki, N., Tytler, D., Kirkman, D., O'Meara, J. M., & Lubin, D. 2005, ApJ, 618, 592
- Thom, C., Peek, J. E. G., Putman, M. E., Heiles, C., Peek, K. M. G., & Wilhelm, R. 2008, ApJ, 684, 364
- Tumlinson, J., et al. 2011, Science, 334, 948
- Tytler, D., Paschos, P., Kirkman, D., Norman, M. L., & Jena, T. 2009, MNRAS, 393, 723
- Vogt, S. S., et al. 1994, in Proc. SPIE Instrumentation in Astronomy VIII, David L. Crawford; Eric R. Craine; Eds., Volume 2198, p. 362, 362–+
- Wakker, B. P., et al. 2007, ApJ, 670, L113
- Wakker, B. P., York, D. G., Wilhelm, R., Barentine, J. C., Richter, P., Beers, T. C., Ivezić, Ž., & Howk, J. C. 2008, ApJ, 672, 298
- Werk, J. K., Prochaska, J. X., Thom, C., Tumlinson, J., Tripp, T. M., O'Meara, J. M., & Peebles, M. S. 2013, ApJS, 204, 17
- Wolfe, A. M., Gawiser, E., & Prochaska, J. X. 2005, ARA&A, 43, 861
- Wotta, C. B., Lehner, N., Howk, J. C., O'Meara, J. M., & Prochaska, J. X. 2016, ApJ, 831, 95

Table 1
HIRES Deckers used in KODIAQ DR1

Decker	Width (arcsec)	Spectra Resolution (FWHM)
B2	0.574	72,000
B5	0.861	48,000
C1	0.861	48,000
C2	0.861	48,000
C5	1.148	36,000
D1	1.148	36,000
E3	0.400	103,000

KODIAQ DR2

Table 2
The KODIAQ DR1 Sample

Object	R.A. ^a (J2000)	Dec. ^a (J2000)	z_{em}^a	Observation Date	PI	Total Exp. Time (s)	Decker	Wavelength Coverage (Å)
J000150–015940	00:01:50.0	−01:59:40	2.810	Sep 1997	Wolfe	25000	C5	4111–6520
J000520+052410	00:05:20.21	+05:24:10.79	1.887	Oct 1999	Sargent	8000	C1	3307–4849
...	Oct 1999	Sargent	8000	C1	3340–4888
...	Sep 1998	Steidel	3600	C1	3217–4723
J001602–001224	00:16:02.40	−00:12:24.9	2.087	Nov 1996	Roth	9000	C1	3766–6191
...	Nov 1996	Roth	5400	C1	3903–6875
J001708+813508	00:17:08.47	+81:35:08.13	3.366	Aug 1995	Cowie	3600	C1	4414–6873
...	Aug 1995	Cowie	5400	C1	4437–6911
...	Nov 1996	Roth	10800	C1	5353–7791
J002208–150539	00:22:08.0	−15:05:39	4.528	Sep 1996	Wolfe	13500	C5	5293–7792
J004434–261121	00:44:34.1	−26:11:21	3.289	Jul 1997	Chaffee	2851	C1	4107–6514
...	Jul 1997	Chaffee	1921	C1	4126–6564
J005233+014040	00:52:33.68	+01:40:40.94	2.307	Nov 1996	Roth	3600	C1	5281–7635
J010054+021136	01:00:54.11	+02:11:36.26	1.959	Oct 1999	Sargent	8000	C1	3317–4849
...	Oct 1999	Sargent	8000	C1	3340–4889
...	Sep 1998	Steidel	14400	C1	3218–4723
J010311+131617	01:03:11.26	+13:16:17.74	2.721	Nov 2002	Wolfe	19800	C1	4475–6896
J010806+163550	01:08:06.41	+16:35:50.0	2.652	Oct 1999	Tytler	31200	C5	3189–4723
...	Sep 2000	Tytler	42700	C5	3189–4724
...	Nov 1999	Wolfe	1800	C5	4218–6655
J012156+144823	01:21:56.03	+14:48:23.8	2.870	Oct 1998	Cowie	12000	C5	3950–6254
...	Oct 1998	Cowie	14400	C5	3970–6203
...	Nov 1999	Sargent	3000	C1	3853–6168
J012227–042127	01:22:27.88	−04:21:27.17	1.953	Jan 1998	Hamann	6000	C1	3400–4913
...	Jan 1998	Hamann	6000	C1	3405–4920
...	Jul 1996	Sargent	6175	C1	3838–6051
...	Oct 1999	Sargent	8000	C1	3316–4849
...	Oct 1999	Sargent	4000	C1	3341–4889
J013301–400628	01:33:01.93	−40:06:28.0	3.023	Oct 1998	Tytler	47938	C5	3339–4899
J013421+330756	01:34:21.6	+33:07:56	4.520	Dec 2003	Hamann	6000	C2	5597–7951
...	Dec 2003	Hamann	3000	C2	6234–8578
J013515–021349	01:35:15.31	−02:13:49.04	1.820	Dec 1997	Becker	7200	C5	3892–6282
J014516–094517	01:45:16.61	−09:45:17.36	2.729	Nov 1999	Sargent	6000	C1	3856–6167
J015227–200107	01:52:27.34	−20:01:07.1	2.147	Sep 1998	Steidel	3600	C1	4117–6528
J015234+335033	01:52:34.57	+33:50:33.15	2.431	Sep 1997	Wolfe	17600	C5	4069–6526
J015741–010629	01:57:41.56	−01:06:29.6	3.564	Dec 2003	Prochaska	9000	C5	4000–6294
...	Aug 2002	Tytler	4400	C5	3937–5508
J020346+113445	02:03:46.65	+11:34:45.40	3.610	Oct 1997	Steidel	40500	C1	4473–6914
J020455+364917	02:04:55.59	+36:49:17.98	2.912	Aug 2001	Tytler	22600	C5	3166–4716
J021857+081727	02:18:57.36	+08:17:27.43	2.995	Aug 1995	Sargent	6600	C1	5229–7653
...	Oct 1995	Sargent	6000	C2	5232–7674
J022839–101110	02:28:39.10	−10:11:10.7	2.256	Jan 1996	Junkkarinen	9000	C1	3760–6181
...	Jan 1996	Junkkarinen	9000	C1	3983–6198
J023145+132254	02:31:45.89	+13:22:54.71	2.059	Sep 1998	Steidel	3600	C1	3218–4723
J023838+163659	02:38:38.93	+16:36:59.27	0.940	Dec 1997	Cohen	4800	C1	3834–6170
...	Dec 1997	Cohen	4800	C1	3918–6178
J024008–230915	02:40:08.17	−23:09:15.77	2.225	Dec 1997	Sargent	6000	C5	3504–5045
...	Dec 1997	Sargent	6000	C5	3504–5044
J024401–013403	02:44:01.84	−01:34:03.7	4.010	Aug 1995	Sargent	4800	C1	4469–6888
...	Aug 1995	Sargent	6600	C1	4493–6921
J024854+180249	02:48:54.25	+18:02:49.5	4.403	Oct 1995	Sargent	7000	C2	6072–8507
...	Oct 1995	Sargent	6000	C2	5929–8387
J025518+004847	02:55:18.58	+00:48:47.6	3.988	Nov 1999	Wolfe	9400	C1	5800–8156
...	Nov 1999	Wolfe	1800	C5	5800–8156
J025625–011911	02:56:25.63	−01:19:11.66	2.490	Dec 1997	Becker	7200	C5	4060–6287
...	Dec 1997	Becker	6600	C5	4030–6423
J025905+001121	02:59:05.64	+00:11:21.8	3.365	Feb 2000	Steidel	3600	C1	4357–6756
...	Feb 2000	Steidel	3600	C1	4381–6789
...	Sep 1999	Steidel	13500	C1	4358–6758
...	Sep 1999	Steidel	13500	C1	4382–6791
...	Sep 1998	Steidel	3600	C1	3806–5353
...	Sep 1998	Steidel	3900	C1	4317–6757
J030341–002321	03:03:41.04	−00:23:21.8	3.175	Dec 2003	Prochaska	7800	C5	3977–6410
J030449–000813	03:04:49.86	−00:08:13.4	3.295	Dec 1996	Cowie	9600	C5	4223–6712
...	Dec 1996	Cowie	11233	C5	4226–6665
J030449–221151	03:04:49.86	−22:11:51.9	1.409	Sep 1998	Steidel	3600	C1	3765–5333
J032412–320259	03:24:12.44	−32:02:59.8	3.302	Dec 1998	Tytler	7400	C5	3820–5357
J033900–013318	03:39:00.9	−01:33:18	3.197	Oct 1999	Tytler	5400	C5	3937–6400
...	Oct 2003	Wolfe	21600	C1	4312–6767
J034943–381031	03:49:43.68	−38:10:31.1	3.222	Sep 1996	Wolfe	14489	C5	4853–7333
J035116+061914	03:51:16.56	+06:19:14.5	2.059	Dec 1998	Hamann	6000	C1	3500–5042
...	Dec 1998	Hamann	6000	C1	3507–5050
J042408+020424	04:24:08.56	+02:04:24.97	2.044	Oct 2001	Cowie	7200	C1	3861–6080
...	Oct 1999	Sargent	8000	C1	3316–4850

Table 2 — *Continued*

Object	R.A. ^a (J2000)	Dec. ^a (J2000)	z_{em}^a	Observation Date	PI	Total Exp. Time (s)	Decker	Wavelength Coverage (Å)
...	Oct 1999	Sargent	8000	C1	3340–4890
J042707–130253	04:27:07.30	−13:02:53.64	2.166	Dec 1998	Hamann	3300	C1	3500–5042
...	Dec 1998	Hamann	3300	C1	3507–5049
...	Jan 1998	Hamann	6000	C1	3466–4980
...	Jan 1998	Hamann	6000	C1	3455–4989
...	Feb 1998	Steidel	7200	C1	4528–6978
J043038–133546	04:30:38.80	−13:35:46.0	3.249	Nov 1999	Sargent	6000	C1	4382–6791
J045142–132033	04:51:42.60	−13:20:33.0	3.093	Dec 1996	Sargent	6000	C1	3722–6183
...	Dec 1997	Sargent	6000	C5	3686–5202
J045312–130546	04:53:12.80	−13:05:46.0	2.300	Feb 1998	Steidel	7200	C1	4253–6721
J045608–215909	04:56:08.93	−21:59:09.54	0.534	Dec 1997	Cohen	3000	C1	3882–6179
J050112–015914	05:01:12.80	−01:59:14.25	2.286	Oct 1995	Wolfe	31240	C5	3889–6298
J053007–250329	05:30:07.96	−25:03:29.84	2.765	Jan 1998	Lu	12000	C1	4115–6527
...	Dec 1997	Sargent	9000	C5	3504–5045
...	Dec 1997	Sargent	9000	C5	3504–5045
J055246–363727	05:52:46.19	−36:37:27.6	2.318	Nov 1996	Roth	3600	C1	4537–7023
...	Nov 1996	Roth	9000	C1	4537–7023
J064204+675835	06:42:04.25	+67:58:35.62	3.177	Dec 2003	Cowie	9600	C5	4173–6541
...	Dec 2003	Cowie	7200	C5	4173–6541
...	Dec 1999	Cowie	4800	C5	4106–6514
...	Oct 1997	Cowie	7200	C5	4174–6541
...	Feb 1995	Sargent	9000	C1	4087–6076
...	Feb 1998	Tytler	19800	C5	3539–5103
...	Oct 1998	Tytler	12600	C5	3470–5036
J064632+445116	06:46:32.02	+44:51:16.58	3.408	Nov 1999	Sargent	6000	C1	4493–5900
J074521+473436	07:45:21.78	+47:34:36.2	3.220	Feb 1999	Cowie	7200	C5	4154–6513
...	Feb 1999	Cowie	7200	C5	4178–6547
...	Feb 1998	Cowie	7200	C5	4176–6544
...	Feb 1998	Cowie	7200	C5	4152–6591
...	Nov 1997	Cowie	7200	C5	3836–6282
...	Nov 1997	Cowie	7200	C5	3845–6295
...	Dec 1998	Tytler	21600	C5	3575–5128
J074711+273903	07:47:11.15	+27:39:03.3	4.154	Oct 2003	Wolfe	1000	D1	5822–8185
J075054+425219	07:50:54.64	+42:52:19.2	1.896	Oct 1999	Sargent	7000	C1	3307–4375
...	Oct 1999	Sargent	6700	C1	3340–4890
...	Mar 2001	Tytler	9000	C5	3027–4582
J080117+521034	08:01:17.79	+52:10:34.5	3.235	Dec 1999	Cowie	7200	C5	4154–6589
...	Feb 1999	Cowie	7200	C5	4154–6513
...	Feb 1999	Cowie	7200	C5	4178–6547
...	April 1999	Sargent	1800	C1	4043–5596
J080342+302254	08:03:42.04	+30:22:54.6	2.030	Oct 2001	Cowie	3600	C1	3849–6080
J080447+101523	08:04:47.96	+10:15:23.7	1.948	Jan 1998	Hamann	6000	C1	3400–4914
...	Jan 1998	Hamann	6000	C1	3406–4920
J081240+320808	08:12:40.68	+32:08:08.6	2.711	Mar 2003	Wolfe	18000	C1	4714–7173
...	Mar 2003	Wolfe	18000	C1	4720–7177
...	Mar 2002	Wolfe	10800	C1	4311–6766
...	Nov 2002	Wolfe	9901	C1	4314–6770
J081336+481302	08:13:36.06	+48:13:02.64	0.870	Nov 1996	Roth	7200	C1	3859–6080
...	Nov 1996	Roth	5400	C1	4100–6078
...	Nov 1999	Wolfe	6600	C5	3857–5978
J083141+524517	08:31:41.70	+52:45:17.5	3.911	April 1998	Chaffee	7200	C1	4423–5952
...	May 1998	Chaffee	2700	C1	4410–5954
...	May 1998	Chaffee	2700	C1	4397–5899
...	Oct 1998	Cowie	6300	C5	5343–7766
...	Oct 1998	Cowie	11400	C5	5301–7783
J083712+145917	08:37:12.89	+14:59:17.3	2.512	Apr 2002	Sargent	4409	C1	3105–4648
J083933+111207	08:39:33.0	+11:12:07	2.696	Mar 2000	Wolfe	9987	C5	4061–6517
J084044+363327	08:40:44.41	+36:33:27.8	1.225	Dec 1997	Becker	6600	C5	3882–6288
...	Dec 1997	Becker	6600	C5	4031–6423
J084424+124548	08:44:24.26	+12:45:46.41	0.072	Nov 1997	Chaffee	7200	C5	4791–7191
...	Dec 1997	Sargent	18000	C5	3403–4917
...	Feb 1998	Wolfe	7200	C5	4778–7174
J084547+132858	08:45:47.19	+13:28:58.2	1.883	Mar 1998	Steidel	7200	C1	3931–6082
J085141+161221	08:51:41.76	+16:12:21.9	1.926	Dec 1998	Hamann	6900	C1	3406–4921
...	Dec 1998	Hamann	6600	C1	3400–4914
...	Jan 1998	Hamann	6600	C1	3406–4921
...	Jan 1998	Hamann	6600	C1	3406–4921
J090033+421546	09:00:33.49	+42:15:46.8	3.290	Dec 1997	Becker	10800	C5	3943–6286
...	May 1997	Becker	3600	C5	3932–6298
...	Mar 2002	Wolfe	7200	C1	5127–7600
J093337+284532	09:33:37.28	+28:45:32.31	3.425	Dec 1997	Sargent	6000	C5	3847–5358
...	Feb 2000	Steidel	14400	C5	4466–6884
...	Feb 2000	Steidel	14400	C5	4438–6890
J093748+730158	09:37:48.91	+73:01:58.1	2.525	Dec 2003	Hamann	6000	C1	4075–6521
...	Feb 1998	Steidel	7200	C1	4901–7307

KODIAQ DR2

Table 2 — *Continued*

Object	R.A. ^a (J2000)	Dec. ^a (J2000)	z_{em}^a	Observation Date	PI	Total Exp. Time (s)	Decker	Wavelength Coverage (Å)
...	Mar 2003	Wolfe	5400	C1	4070–6514
J093857+412821	09:38:57.01	+41:28:21.2	1.935	Jan 1998	Hamann	6300	C1	3401–4914
...	Jan 1998	Hamann	3300	C1	3406–4921
...	Apr 2002	Sargent	3000	C1	3108–4646
J095122+263513	09:51:22.57	+26:35:13.9	1.246	April 1999	Sargent	1800	C1	3584–5129
J095355–050418	09:53:55.70	−05:04:18.0	0.000	Apr 1997	Wolfe	30600	D1	6031–8388
J095500–013000	09:55:00	−01:30:00.0	4.500	Mar 1999	Wolfe	28800	D1	5706–8155
J095714+544017	09:57:14.67	+54:40:17.5	2.589	Feb 1998	Steidel	7200	C1	4162–6525
J095852+120245	09:58:52.19	+12:02:45.0	3.297	Apr 1997	Cowie	4800	C5	4337–6774
...	Nov 1999	Sargent	5100	C1	4382–6792
J100110+552834	10:01:10.17	+55:28:34.68	2.102	Feb 1998	Steidel	7200	C1	4162–6525
J100120+555355	10:01:20.69	+55:53:55.61	1.414	Jan 1998	Lu	12000	C1	4305–6757
...	Jan 1998	Lu	17000	C1	4327–6777
...	Dec 1997	Sargent	26600	C5	3504–5045
...	Dec 1997	Sargent	9000	C5	3504–5045
J100205+554257	10:02:05.36	+55:42:57.9	1.150	Dec 1997	Cohen	3300	C1	3840–6179
...	Dec 1997	Cohen	3300	C1	3996–6191
J100841+362319	10:08:41.22	+36:23:19.3	3.125	Mar 2001	Tytler	21200	C5	3542–5059
J101155+294141	10:11:55.60	+29:41:41.6	2.652	Jan 1996	Sargent	5379	C1	3945–6076
...	Jun 2003	Sargent	6000	C1	4582–7020
...	Jun 2003	Sargent	6000	C1	4612–7050
J101549+002019	10:15:49.00	+00:20:19.9	4.402	Mar 2002	Wolfe	5400	C2	6215–8554
J101556–003504	10:15:56.32	−00:35:04.9	2.462	Feb 1998	Wolfe	16200	D1	6210–8549
J102009+104002	10:20:09.99	+10:40:02.7	3.167	May 1996	Cowie	4800	C5	3806–6084
...	Dec 2003	Hamann	9000	C1	4075–6523
J102156+300140	10:21:56.56	+30:01:40.4	3.129	Mar 2002	Wolfe	7200	C1	4722–7185
J103456+035859	10:34:56.31	+03:58:59.3	3.369	May 1996	Cowie	7200	C5	4045–6089
J104117+061016	10:41:17.16	+06:10:16.92	1.270	Mar 1998	Steidel	7200	C1	3975–6408
J104459+365605	10:44:59.60	+36:56:05.1	0.700	Dec 1997	Becker	7200	C5	3847–6284
...	May 1997	Becker	3600	C5	3892–6084
J105427+253600	10:54:27.18	+25:36:00.8	2.400	Dec 1997	Becker	3000	C5	3882–6288
...	Dec 1997	Becker	3000	C5	4031–6424
J105756+455553	10:57:56.28	+45:55:53.0	4.137	Feb 1998	Cowie	7200	C5	3927–6393
...	Feb 1998	Cowie	7200	C5	3936–6391
...	Feb 1998	Cowie	7200	C5	5590–7942
...	May 1996	Sargent	6000	C1	5637–8003
...	May 1996	Sargent	6000	C1	4607–7054
...	May 1996	Sargent	6000	C1	4586–7025
J110610+640009	11:06:10.74	+64:00:09.6	2.202	Apr 1997	Tytler	7200	C5	3168–4713
J111038+483115	11:10:38.64	+48:31:15.7	2.954	Feb 1995	Sargent	6000	C1	3926–6076
J111113–080402	11:11:13.6	−08:04:02	3.922	Mar 1999	Wolfe	12600	D1	6060–8348
J112442–170517	11:24:42.87	−17:05:17.5	2.397	Feb 1998	Cowie	6300	C5	3952–6095
...	Feb 1998	Cowie	6300	C5	3940–6141
...	Apr 1997	Tytler	10800	C5	3167–4713
J114308+345222	11:43:08.88	+34:52:22.3	3.145	Mar 1999	Sargent	12000	C1	4306–6758
...	Mar 1999	Sargent	9000	C1	4224–6663
J115944+011207	11:59:44.81	+01:12:07.0	2.002	Mar 2002	Wolfe	25000	C1	3848–6160
J120006+312630	12:00:06.25	+31:26:30.8	2.989	Apr 1997	Tytler	7200	C5	3436–4985
...	Jan 1997	Tytler	18600	C5	3969–6178
J120247+120630	12:02:48.09	+12:07:13.94	0.638	Apr 1997	Cowie	7200	C5	4643–7126
...	Apr 1997	Cowie	7200	C5	4672–7059
J120917+113830	12:09:17.93	+11:38:30.3	3.105	Feb 1999	Cowie	9600	C5	3970–6400
...	Feb 1999	Cowie	9600	C5	3984–6411
J121134+090220	12:11:34.95	+09:02:20.8	3.291	Mar 2003	Wolfe	10800	C1	4068–6507
J121303+171423	12:13:03.02	+17:14:23.3	2.558	Mar 2000	Wolfe	7200	C5	3802–6184
J121930+494052	12:19:30.77	+49:40:52.3	2.633	Feb 2003	Sargent	2800	C1	3884–6182
...	Feb 2003	Sargent	3919	C1	3772–6200
...	Jun 2003	Sargent	6000	C1	4582–7020
...	Jun 2003	Sargent	6000	C1	4612–7052
J122137+043026	12:21:37.94	+04:30:26.1	0.094	April 1999	Sargent	4600	C1	3585–5130
J122607+173649	12:26:07.19	+17:36:49.9	2.924	Feb 1998	Wolfe	10100	C5	4784–7181
J122824+312837	12:28:24.96	+31:28:37.62	2.200	April 1999	Sargent	12000	C1	3118–4530
J123200–022404	12:32:00.01	−02:24:04.79	1.043	Apr 1997	Smith	6000	C1	3369–4908
...	Apr 1997	Smith	6000	C1	3372–4909
J124610+303117	12:46:10.8	+30:31:17	2.560	April 1999	Tytler	23400	C5	3160–4698
...	Mar 2000	Tytler	32400	C5	3161–4711
J124913–055918	12:49:13.86	−05:59:18.9	2.226	Mar 1998	Steidel	7200	C1	3931–6293
J125005+263107	12:50:05.72	+26:31:07.5	2.047	Feb 1998	Steidel	5400	C1	3889–6281
J130554+303252	13:05:54.72	+30:32:52.29	1.759	April 1998	Chaffee	17400	C1	3470–5030
...	Jun 2003	Chaffee	18900	C1	3470–5028
...	May 1998	Chaffee	10800	C1	3475–4985
J131011+460124	13:10:11.61	+46:01:24.5	2.133	April 1999	Sargent	6000	C1	3569–5119
...	April 1999	Sargent	3000	C1	3317–4849
...	April 1999	Sargent	4600	C1	3123–4526
...	April 1999	Sargent	3000	C1	3316–4852

Table 2 — *Continued*

Object	R.A. ^a (J2000)	Dec. ^a (J2000)	z_{em}^a	Observation Date	PI	Total Exp. Time (s)	Decker	Wavelength Coverage (Å)
J131215+423900	13:12:15.23	+42:39:00.8	2.566	Feb 1998	Cowie	7800	C5	3953–6068
...	Feb 1998	Cowie	7800	C5	3964–6061
J133108+303032	13:31:08.29	+30:30:32.9	0.849	Apr 1997	Smith	6000	C1	3369–4908
...	Apr 1997	Smith	2350	C1	3159–4660
...	Apr 1997	Smith	6000	C1	3372–4908
J134002+110630	13:40:02.54	+11:06:30.2	2.913	Mar 2000	Wolfe	8100	C5	4660–7044
J134004+281653	13:40:04.95	+28:16:53.3	2.517	Apr 1997	Tytler	7200	C5	3160–4711
J134916–033715	13:49:16.7	−03:37:15	3.992	Apr 1997	Wolfe	30200	D1	5897–8347
J135038–251216	13:50:38.88	−25:12:16.8	2.534	Apr 2002	Sargent	7200	C1	3109–4648
J135405+313902	13:54:05.39	+31:39:02.3	1.320	Mar 1998	Steidel	12200	C1	3988–6160
J142438+225600	14:24:38.09	+22:56:00.59	3.620	Feb 1999	Cowie	20400	C5	4766–7156
...	Feb 1999	Cowie	19200	C5	4800–7203
...	Jul 1995	Cowie	13200	C5	4711–7156
...	May 1996	Cowie	9600	C5	4865–7202
...	Apr 1998	Sargent	9000	B2	4154–6592
...	Apr 1998	Sargent	9000	B2	4174–6541
...	Apr 1998	Sargent	9000	B2	4831–7297
...	April 1999	Sargent	12000	C5	3569–5119
...	April 1999	Sargent	9000	C5	3583–5130
...	Feb 1995	Sargent	6000	C5	3989–6076
J142656+602550	14:26:56.19	+60:25:50.7	3.191	Mar 2002	Wolfe	4500	C2	5616–7975
J143912+295448	14:39:12.34	+29:54:48.0	2.992	Mar 1998	Sargent	10680	C1	3575–5121
J144331+272436	14:43:31.17	+27:24:36.7	4.443	Mar 1999	Wolfe	25200	D1	6070–8482
J144453+291905	14:44:53.54	+29:19:05.58	2.660	Jun 1995	Sargent	5400	C1	3872–6076
...	Jun 1995	Sargent	5100	C1	3830–6083
J144516+095836	14:45:16.46	+09:58:36.1	3.529	Jul 1997	Chaffee	9000	C1	4126–6542
...	Jul 1997	Chaffee	9000	C1	4105–6512
J152144+525449	15:21:44.8	+52:54:49	1.855	Apr 1998	Sargent	12000	B2	4154–6592
...	Apr 1998	Sargent	9000	B2	4233–6541
J155152+191104	15:51:52.48	+19:11:04.2	2.843	Mar 1999	Sargent	24000	C1	3645–6078
...	Mar 1999	Sargent	21000	C1	3895–6091
J155610+374039	15:56:10.60	+37:40:39.6	2.658	Apr 1997	Tytler	9000	C5	3247–4775
J155855+332318	15:58:55.19	+33:23:18.6	1.654	April 1998	Chaffee	4800	C1	3841–5029
...	May 1998	Chaffee	8100	C1	3477–4985
J160355+573054	16:03:55.93	+57:30:54.41	2.850	April 1999	Tytler	27660	C5	3306–4599
...	May 2000	Tytler	14400	C5	3209–4602
J160455+381201	16:04:55.39	+38:12:01.65	2.551	Apr 2002	Sargent	3600	C1	3105–4646
...	Apr 2002	Sargent	3600	C1	3109–4647
...	Jun 2003	Sargent	6000	C1	4583–7020
...	Jun 2003	Sargent	6000	C1	4612–7053
J162548+264433	16:25:48.0	+26:44:33	2.535	May 1996	Cowie	7200	C5	3970–5976
...	Aug 1995	Sargent	6000	C1	3972–6076
...	May 1996	Sargent	9000	C1	3883–6076
J162548+264658	16:25:48.79	+26:46:58.7	2.517	May 1996	Cowie	9600	C5	3923–5974
...	Aug 1995	Sargent	6000	C1	3841–6076
J162557+264448	16:25:57.38	+26:44:48.2	2.601	Jul 1996	Sargent	6000	C1	4011–6052
...	May 1996	Sargent	6000	C1	3971–6076
J162645+642655	16:26:45.69	+64:26:55.2	2.320	Jun 2001	Cowie	9600	C5	3801–6078
...	Jul 1996	Sargent	6000	C1	3845–6053
...	Jul 1996	Sargent	4863	C1	3811–6010
J163412+320335	16:34:12.78	+32:03:35.5	2.343	Jun 2001	Cowie	7200	C5	3903–6077
...	Jun 2001	Cowie	7200	C5	4547–5993
J164656+551446	16:46:56.40	+55:14:46.2	4.050	Mar 2001	Tytler	15000	C5	4541–6076
J170100+641209	17:01:00.61	+64:12:09.0	2.734	May 1996	Cowie	9600	C5	3806–5969
...	Apr 2002	Sargent	4617	C1	3109–4647
...	April 1999	Sargent	7800	C1	3318–4849
...	April 1999	Sargent	4200	C1	3319–4852
...	May 1996	Sargent	8000	C1	3996–6076
J170124+514920	17:01:24.82	+51:49:20.40	0.292	Apr 1997	Smith	5200	C1	3159–4660
J170919+281835	17:09:19.9	+28:18:35	2.370	May 1998	Becker	3000	C5	3885–6291
...	May 1998	Becker	3000	C5	3894–6304
J171938+480412	17:19:38.24	+48:04:12.24	1.083	May 2000	Tytler	5000	C5	3403–4955
J175746+753916	17:57:46.35	+75:39:16.17	3.050	Jul 1997	Chaffee	6000	C1	4106–6514
...	Jul 1997	Chaffee	9000	C1	4127–6543
...	Jul 1997	Chaffee	6000	C1	4126–6563
...	Sep 1996	Wolfe	10444	C1	5170–7591
J185230+401906	18:52:30.37	+40:19:06.60	2.120	Jul 1996	Sargent	6000	C1	3806–6190
J193957–100241	19:39:57.25	−10:02:41.54	3.787	Oct 1997	Cowie	15773	C5	4018–6405
J194455+770552	19:44:55.0	+77:05:52	3.02	Jun 2001	Cowie	7200	C5	3926–6362
...	Jun 2001	Cowie	9600	C5	3941–6379
...	Oct 1998	Cowie	9600	C5	3925–6380
...	Oct 1998	Cowie	9093	C5	3984–6396
...	May 1998	Tytler	15970	C5	3470–4985

KODIAQ DR2

Table 2 — *Continued*

Object	R.A. ^a (J2000)	Dec. ^a (J2000)	z_{em}^a	Observation Date	PI	Total Exp. Time (s)	Decker	Wavelength Coverage (Å)
...	Oct 1998	Tytler	24000	C5	3488–5039
J200324–325145	20:03:24.11	−32:51:45.02	3.783	Aug 1995	Cowie	7200	C5	5386–7835
J204051–010538	20:40:51.40	−01:05:38.0	2.783	Aug 2002	Tytler	14400	C5	3341–4854
J211452+060742	21:14:52.59	+06:07:42.33	0.457	Nov 1996	Roth	1800	C1	3805–5976
J212912–153841	21:29:12.17	−15:38:41.02	3.268	Jul 1995	Cowie	15900	C5	3879–6188
J213135–120704	21:31:35.26	−12:07:04.79	0.501	Aug 1995	Sargent	2500	C1	3841–6076
J215502+135826	21:55:02.2	+13:58:26	4.260	Sep 1999	Djorgovski	5400	C5	4255–6635
...	Sep 1999	Djorgovski	3000	C5	4223–6662
...	Sep 1999	Djorgovski	2400	C5	4274–6662
J220852–194400	22:08:52.07	−19:44:00.0	2.573	Nov 1999	Sargent	6000	C1	3909–6165
...	Oct 1999	Sargent	8000	C1	3319–4849
...	Oct 1999	Sargent	12000	C1	3340–4890
J221516–294423	22:15:16.03	−29:44:23.33	2.706	July 1996	Chaffee	6600	C1	3978–5998
J221527–161132	22:15:27.31	−16:11:32.9	3.990	Aug 1995	Sargent	6000	C1	4469–6888
...	Aug 1995	Sargent	6000	C1	4492–6921
J221852–033536	22:18:52.03	−03:35:36.87	0.901	Sep 1998	Steidel	3600	C1	3847–5357
J222547–045701	22:25:47.26	−04:57:01.39	1.404	Nov 1996	Roth	3600	C1	3722–6078
J223235+024755	22:32:35.23	+02:47:55.8	2.147	Sep 1997	Wolfe	12600	C5	3882–6287
...	Sep 1997	Wolfe	5400	C5	4415–6879
J223408+000001	22:34:08.98	+00:00:01.73	3.027	Oct 1995	Wolfe	15300	C5	3976–6409
J223619+132620	22:36:19.19	+13:26:20.3	3.295	Jul 1996	Sargent	6000	C1	4898–7303
...	Jul 1996	Sargent	9000	C1	4899–7304
J223627+135714	22:36:27.07	+13:57:14.0	3.216	Sep 1999	Steidel	36000	C1	4154–6630
...	Sep 1999	Steidel	32400	C1	4174–6618
J223953–055219	22:39:53.66	−05:52:19.9	4.558	Dec 2003	Cowie	9000	C1	5735–8194
...	Aug 1995	Sargent	12000	C1	4968–7304
...	Aug 1995	Sargent	12000	C1	4934–7350
J224030+032130	22:40:30.3	+03:21:30	1.695	Jan 1998	Lu	5250	C1	3969–6399
...	Jan 1998	Lu	5300	C1	3940–6407
J230444+031145	23:04:44.95	+03:11:45.80	1.052	Jul 1996	Sargent	3000	C1	3843–6050
...	Oct 1999	Sargent	1800	C1	3340–4889
J234023–005327	23:40:23.66	−00:53:27.0	2.085	Oct 2003	Wolfe	3600	C5	3894–6305
J234451+343348	23:44:51.25	+34:33:48.64	3.010	Oct 2003	Wolfe	7200	C5	4646–7127
J234531+090906	23:45:31.0	+09:09:06.0	2.784	Oct 1997	Steidel	11200	C1	3804–6272
J234628+124859	23:46:28.2	+12:48:59.00	2.573	Dec 1996	Sargent	6000	C2	6522–8934
...	Oct 1995	Sargent	6000	C2	3861–6065
...	Oct 1995	Sargent	3000	C2	3876–6062
...	Sep 1998	Steidel	3600	C1	3370–4917
...	Sep 1998	Steidel	7200	C1	3575–5117
J234632+124540	23:46:32.80	+12:45:40.0	2.515	Oct 1995	Sargent	6000	C1	3858–6066
...	Oct 1995	Sargent	9000	C1	3846–6064
J235010+081255	23:50:10.07	+08:12:55.27	1.700	Oct 2001	Cowie	1728	C5	3979–6081
J235057–005209	23:50:57.87	−00:52:09.9	3.025	Nov 1997	Chaffee	10800	C5	5067–7494
...	Nov 1997	Cowie	14400	C1	3897–6308
...	Nov 1999	Wolfe	10800	C5	5062–7487
...	Nov 1999	Wolfe	3989	C5	5067–7494
J235129–142756	23:51:29.81	−14:27:56.9	2.933	Sep 1996	Wolfe	13500	C5	3846–6296
J235953–124148	23:59:53.64	−12:41:48.2	0.868	Dec 1997	Becker	3000	C5	5038–7455
...	Dec 1997	Becker	3000	C5	4317–6774

Note. — ^aJ2000 coordinates and quasar redshifts are determined by passing the quasar coordinates from the raw data header through SIMBAD or SDSS and choosing the appropriate match.

Table 3
The KODIAQ DR2 Sample

Object	z_{em}	Total Exp, Time (s)	Wavelength Coverage (Å)	Rest Wavelength Coverage (Å) ^b
J000150-015940	2.81	25000	4111–6520	1079–1711
J000520+052410	1.887	19600	3217–4888	1114–1693
J000931+021707	2.35	1200	3334–6198	995–1850
J001602-001224	2.087	14400	3766–6875	1219–2227
J001708+813508	3.366	19800	4414–7791	1010–1784
J002127-020333	2.596	700	3366–6198	936–1723
J002208-150539	4.528	13500	5293–7792	957–1409
J002830-281704	2.4	600	3366–6198	989–1822
J002952+020606	2.333	1000	3367–6198	1010–1859
J003501-091817	2.418	16200	3123–5980	913–1749
J004054-091526	4.976	7200	5453–8570	912–1434
J004351-265128	2.786	1500	3370–6198	890–1637
J004358-255115	2.501	900	3365–6198	961–1770
J004434-261121	3.289	4772	4107–6564	957–1530
J004448+372114	2.41	900	3368–6198	987–1817
J004530-261709	3.44	14400	3973–8543	894–1924
J005202+010129	2.27	1000	3366–6198	1029–1895
J005233+014040	2.307	3600	5281–7635	1596–2308
J005700+143737	2.643	1100	3366–6198	923–1701
J005814+011530	2.494	4800	3368–6250	963–1788
J010054+021136	1.959	30400	3218–4889	1087–1652
J010311+131617	2.721	27000	3123–6896	839–1853
J010741-263328	2.46	900	3133–6031	905–1743
J010806+163550	2.652	97904	3048–6655	834–1822
J010925-210257	3.226	5400	3304–6179	781–1462
J011150+140141	2.47	900	3133–6031	902–1738
J012156+144823	2.87	60600	3244–6254	838–1616
J012227-042127	1.953	30175	3316–6051	1122–2049
J013301-400628	3.023	47938	3339–4899	829–1217
J013340+040059	4.15	7200	4159–8742	807–1697
J013421+330756	4.52	9000	5597–8578	1013–1553
J013515-021349	1.82	7200	3892–6282	1380–2227
J014516-094517	2.729	49000	3022–6167	810–1653
J014944+150106	2.07	1200	3176–6038	1034–1966
J015227-200107	2.147	4440	3177–6528	1009–2074
J015234+335033	2.431	17600	4069–6526	1185–1902
J015741-010629	3.564	13400	3937–6294	862–1379
J020346+113445	3.61	40500	4473–6914	970–1499
J020455+364917	2.912	33900	3157–6384	807–1631
J020944+051714	4.18	69300	5193–8319	1002–1605
J020950-000506	2.828	26930	3022–9219	789–2408
J021129+124110	2.953	10200	3681–6588	931–1666
J021857+081727	2.995	12600	5229–7674	1308–1920
J022554+005451	2.975	10800	3571–6485	898–1631
J022839-101110	2.256	18000	3760–6198	1154–1903
J022853-033737	2.066	800	3177–6039	1036–1969
J023145+132254	2.059	5000	3176–6039	1038–1974
J023359+004938	2.522	1080	3174–6033	901–1712
J023838+163659	0.94	9600	3834–6178	1976–3184
J023924-090138	2.471	1080	3133–6032	902–1737
J024008-230915	2.225	12000	3504–5045	1086–1564
J024401-013403	4.01	11400	4469–6921	892–1381
J024854+180249	4.403	13000	5929–8507	1097–1574
J025127+341442	2.23	780	3133–6031	969–1867
J025515+014828	2.47	840	3157–6030	909–1737
J025518+004847	3.988	11200	5800–8156	1162–1635
J025625-011911	2.49	13800	4030–6423	1154–1840
J025644+001246	2.251	900	3157–6030	971–1854
J025905+001121	3.365	41700	3806–6791	871–1555
J030046+022245	2.52	900	3133–6033	890–1713
J030341-002321	3.175	15000	3536–6423	846–1538
J030449-000813	3.295	20833	4226–6712	983–1562
J030449-221151	1.409	3600	3765–5333	1562–2213
J031003-004645	2.114	1200	3133–6032	1006–1937
J032412-320259	3.302	7400	3820–5357	887–1245
J033900-013318	3.197	43300	3686–7198	878–1715
J034943-381031	3.222	14489	4853–7333	1149–1736
J035116+061914	2.059	12000	3500–5050	1144–1650
J040241-064124	2.432	3600	2995–5882	872–1713
J042408+020424	2.044	23200	3316–6080	1089–1997
J042707-130253	2.166	25800	3455–6978	1091–2204
J043038-133546	3.249	6000	4382–6791	1031–1598
J045142-132033	3.093	12000	3686–6183	900–1510
J045213-164012	2.684	17400	3100–5979	841–1622

Table 3 — *Continued*

Object	z_{em}	Total Exp. Time (s)	Wavelength Coverage (Å)	Rest Wavelength Coverage (Å) ^b
J045312-130546	2.3	7200	4253–6721	1288–2036
J045608-215909	0.534	3000	3882–6179	2530–4028
J050112-015914	2.286	31240	3889–6298	1183–1916
J053007-250329	2.765	30000	3504–6527	930–1733
J055246-363727	2.318	12600	4537–7023	1367–2116
J064204+675835	3.177	70200	3470–6541	830–1565
J064632+445116	3.408	6000	4493–5900	1019–1338
J073149+285448	3.675	7200	4160–8768	889–1875
J074110+311200	0.631	1800	3076–5934	1885–3638
J074521+473436	3.22	69300	3575–6591	847–1561
J074711+273903	4.154	1000	5822–8185	1129–1588
J074749+443417	4.435	14400	4850–9459	892–1740
J074927+415242	3.111	12600	3571–8127	868–1976
J075054+425219	1.896	22700	3027–4890	1045–1688
J080117+521034	3.235	41400	4043–6759	954–1595
J080342+302254	2.03	3600	3849–6080	1270–2006
J080447+101523	1.948	12000	3400–4920	1153–1668
J080518+614423	3.033	5400	3987–8534	988–2116
J081240+320808	2.711	71101	3331–7177	897–1933
J081336+481302	0.87	19200	3857–6080	2062–3251
J081435+502946	3.883	21600	4024–9725	824–1991
J081740+135134	4.389	7200	4935–8006	915–1485
J082107+310751	2.625	16420	3058–5981	843–1649
J082540+354414	3.846	10800	5180–9716	1068–2004
J082619+314848	3.093	7900	3842–8362	938–2043
J082849+085854	2.271	1293	3153–5992	963–1831
J083052+241059	0.941	1800	3051–5936	1571–3058
J083102+335803	2.427	18600	3123–5979	911–1744
J083141+524517	3.911	30300	4397–7783	895–1584
J083712+145917	2.512	4409	3105–4648	884–1323
J083933+111207	2.696	9987	4061–6517	1098–1763
J084044+363327	1.225	13200	3882–6423	1744–2886
J084424+124548	0.072	32400	3403–7191	3174–6708
J084547+132858	1.883	7200	3931–6082	1363–2109
J085141+161221	1.926	26100	3400–4921	1161–1681
J090033+421546	3.29	28354	3545–8085	826–1884
J092708+582319	1.91	21600	2995–5880	1029–2020
J092759+154321	1.805	16400	3074–5967	1095–2127
J092914+282529	3.399	10800	4306–7424	978–1687
J093337+284532	3.425	34800	3847–6890	869–1557
J093643+292713	2.923	7200	2995–5869	763–1496
J093748+730158	2.525	18600	4070–7307	1154–2072
J093857+412821	1.935	12600	3108–4921	1058–1676
J094202+042244	3.275	7200	3364–6200	786–1450
J095122+263513	1.246	1800	3584–5129	1595–2283
J095309+523029	1.875	7200	3156–6039	1097–2100
J095355-050418	0.0	30600	6031–8388	6031–8388
J095500-013000	4.5	28800	5706–8155	1037–1482
J095714+544017	2.589	7200	4162–6525	1159–1818
J095820+322402	0.53	600	3078–5934	2011–3878
J095822+014524	1.96	3600	3169–6030	1070–2037
J095852+120245	3.297	18900	3608–8564	839–1993
J100110+552834	2.102	7200	4162–6525	1341–2103
J100120+555355	1.414	64600	3504–6777	1451–2807
J100205+554257	1.15	6600	3840–6191	1786–2879
J100841+362319	3.125	32000	3542–7993	858–1937
J101155+294141	2.652	49194	3048–7050	834–1930
J101336+561536	3.632	3600	3899–8368	841–1806
J101447+430030	3.125	8700	3500–7057	848–1710
J101549+002019	4.402	5400	6215–8554	1150–1583
J101556-003504	2.462	16200	6210–8549	1793–2469
J101723-204658	2.545	14400	3128–5981	882–1687
J101939+524627	2.17	7200	3118–5974	983–1884
J102009+104002	3.167	21000	3616–6524	867–1565
J102156+300140	3.129	7200	4722–7185	1143–1740
J102325+514251	0.597	6200	3584–7975	2244–4993
J102410+060013	2.13	3300	3128–5992	999–1914
J103456+035859	3.369	7200	4045–6089	925–1393
J103514+544040	2.989	14400	3299–7801	827–1955
J104018+572448	3.408	8100	3794–6657	860–1510
J104117+061016	1.27	7200	3975–6408	1751–2822
J104213+062853	2.035	2400	3128–5992	1030–1974
J104459+365605	0.7	10800	3847–6284	2262–3696
J105123+354534	4.912	7800	5127–9713	867–1642
J105427+253600	2.4	6000	3882–6424	1141–1889

Table 3 — *Continued*

Object	z_{em}	Total Exp. Time (s)	Wavelength Coverage (Å)	Rest Wavelength Coverage (Å) ^b
J105648+120826	1.923	21300	3074–5975	1051–2044
J105756+455553	4.137	40800	3927–8003	764–1557
J110045+112239	4.706	17400	5362–8391	939–1470
J110610+640009	2.202	12000	3128–5981	976–1867
J110621+104432	1.859	2700	3325–6184	1162–2162
J111038+483115	2.954	6000	3926–6076	992–1536
J111113-080402	3.922	19800	4158–8751	844–1777
J111909+211917	1.183	1800	3051–5932	1397–2717
J112442-170517	2.397	39000	3126–6141	920–1807
J113130+604420	2.921	7200	3597–6423	917–1638
J113418+574204	3.521	6300	3973–8534	878–1887
J113508+222715	2.886	17600	3433–6311	883–1624
J114308+345222	3.145	18000	4224–6758	1019–1630
J115538+053050	3.475	7200	5057–8140	1130–1818
J115940-003203	2.035	1200	3154–5992	1039–1974
J115944+011207	2.002	25000	3848–6160	1281–2051
J120006+312630	2.989	25800	3436–6178	861–1548
J120147+120630	3.509	14400	4643–7126	1029–1580
J120207+323538	5.292	14400	5123–9709	814–1543
J120416+022111	2.529	10800	3455–6422	979–1819
J120917+113830	3.105	26400	3500–6411	852–1561
J121117+042222	2.526	9000	3403–6302	965–1787
J121134+090220	3.291	10800	4068–6507	948–1516
J121303+171423	2.558	7200	3802–6184	1068–1738
J121930+494052	2.633	31719	3027–7052	833–1941
J122137+043026	0.094	4600	3585–5130	3276–4689
J122518+483116	3.09	9000	3571–8128	873–1987
J122607+173649	2.924	10100	4784–7181	1219–1830
J122824+312837	2.2	19200	3101–5980	969–1868
J123200-022404	1.043	12000	3369–4909	1649–2402
J123643-020420	1.864	3000	3303–6185	1153–2159
J123748+012606	3.144	4000	3370–6274	813–1513
J124610+303117	2.56	55800	3160–4711	887–1323
J124610+303131	2.56	3600	3189–6086	895–1709
J124913-055918	2.226	7200	3931–6293	1218–1950
J124924-023339	2.116	4800	3075–5966	986–1914
J125005+263107	2.047	5400	3889–6281	1276–2061
J130411+295348	2.85	7200	2996–5871	778–1524
J130426+120245	2.98	9000	3606–8171	906–2053
J130542+092427	2.062	5400	3128–5992	1021–1956
J130554+303252	1.759	52500	3470–5030	1257–1823
J131011+460124	2.133	16600	3123–5119	996–1633
J131040+542449	1.929	10800	3244–6136	1107–2094
J131215+423900	2.566	25287	3102–6068	869–1701
J131341+144140	1.884	10800	3243–6132	1124–2126
J131855+531207	2.321	3600	3838–6899	1155–2077
J133108+303032	0.849	14350	3159–4908	1708–2654
J133532+082404	1.909	3000	3326–6185	1143–2126
J134002+110630	2.913	8100	4660–7044	1190–1800
J134004+281653	2.517	7200	3160–4711	898–1339
J134328+572147	3.034	7200	3075–6190	762–1534
J134544+262506	2.031	4800	3501–6386	1155–2106
J134916-033715	3.992	30200	5897–8347	1181–1672
J135038-251216	2.534	13200	3109–5981	879–1692
J135317+532825	2.92	8400	3497–7985	892–2036
J135405+313902	1.32	12200	3988–6160	1718–2655
J140501+444800	2.218	17600	3215–6095	999–1894
J141719+413237	2.023	25200	3281–6188	1085–2046
J141906+592312	2.32	7200	3108–5966	936–1796
J142438+225600	3.62	114000	3569–7297	772–1579
J142656+602550	3.191	4500	5616–7975	1340–1902
J143316+313126	2.94	6000	3245–6095	823–1546
J143500+535953	2.635	7200	3472–6379	955–1754
J143912+295448	2.992	10680	3575–5121	895–1282
J143916-015627	2.162	5400	3075–5967	972–1887
J144331+272436	4.443	25200	6070–8482	1115–1558
J144453+291905	2.66	34900	2995–6083	818–1662
J144516+095836	3.529	18000	4105–6542	906–1444
J145408+511443	3.635	1800	4075–8565	879–1847
J145435+094100	1.945	2400	3152–5992	1070–2034
J150932+111313	2.11	5194	3128–5992	1005–1926
J151224+465233	3.359	11702	3588–6423	823–1473
J152144+525449	1.855	21000	4154–6592	1454–2308
J152156+520238	2.208	7200	3102–5982	966–1864
J154153+315329	2.557	4800	4417–7480	1241–2102

Table 3 — *Continued*

Object	z_{em}	Total Exp. Time (s)	Wavelength Coverage (Å)	Rest Wavelength Coverage (Å) ^b
J155152+191104	2.843	51900	2995–6091	779–1584
J155556+480015	3.298	21600	4018–8565	934–1992
J155610+374039	2.658	9000	3247–4775	887–1305
J155810-003120	2.827	14900	3335–6201	871–1620
J155814+405337	2.635	25200	3101–5979	853–1644
J155855+332304	1.654	12900	3477–5029	1310–1894
J160355+573054	2.85	42060	3209–4602	833–1195
J160413+395121	3.13	10300	4291–8767	1038–2122
J160455+381201	2.551	19200	3105–7053	874–1986
J160455+381214	2.551	17200	3030–5981	853–1684
J160547+511330	1.786	7200	3118–5975	1119–2144
J160843+071508	2.877	12300	3078–7586	793–1956
J161009+472444	3.216	14100	3834–8507	909–2017
J162453+375806	3.38	7200	3561–6591	813–1504
J162548+264433	2.535	43200	3022–8103	854–2292
J162548+264658	2.517	38400	3022–6084	859–1729
J162557+264448	2.601	40489	3102–8123	861–2255
J162645+642655	2.32	35603	3127–6078	941–1830
J162902+091322	1.985	2400	3153–5992	1056–2007
J163412+320335	2.343	14400	3903–6077	1167–1817
J164656+551446	4.05	15000	4541–6076	899–1203
J170100+641209	2.734	61817	3060–8125	819–2175
J170124+514920	0.292	5200	3159–4660	2445–3606
J170919+281835	2.37	6000	3885–6304	1152–1870
J171227+575507	3.008	14700	3451–6310	861–1574
J171938+480412	1.083	5000	3403–4955	1633–2378
J173352+540030	3.424	10800	3735–8543	844–1931
J175603+574848	2.11	61000	3157–8544	1015–2747
J175746+753916	3.05	40444	4106–7591	1013–1874
J182157+642036	0.297	2400	3105–5932	2393–4573
J185230+401906	2.12	6000	3806–6190	1219–1983
J193957-100241	3.787	56173	3569–6759	745–1411
J194455+770552	3.02	75463	3470–6396	3470–6396
J200324-325145	3.783	19200	3565–8300	745–1735
J203642-055300	2.582	21600	3244–8565	905–2391
J204051-010538	2.783	14400	3341–4854	883–1283
J210025-064146	3.137	30660	3722–8981	899–2170
J211452+060742	0.457	1800	3805–5976	2611–4101
J212329-005052	2.262	21600	3027–5896	927–1807
J212904-160249	2.9	14400	3992–8545	1023–2191
J212912-153841	3.268	23100	3571–6422	836–1504
J213135-120704	0.501	2500	3841–6076	2558–4047
J215502+135826	4.26	10800	4223–6662	802–1266
J220639-181846	2.728	5400	3304–6183	886–1658
J220852-194400	2.573	38000	3022–6165	845–1725
J221516-294423	2.706	6600	3978–5998	1073–1618
J221527-161132	3.99	12000	4469–6921	895–1386
J221852-033536	0.901	3600	3847–5357	2023–2817
J222256-094636	2.926	10800	3214–6096	818–1552
J222547-045701	1.403	3600	3722–6078	1548–2529
J223235+024755	2.147	18000	3882–6879	1233–2185
J223408+000001	3.027	15300	3976–6409	987–1591
J223619+132620	3.295	15000	4898–7304	1140–1700
J223627+135714	3.216	68400	4154–6630	985–1572
J223953-055219	4.558	33000	4934–8194	887–1474
J224030+032130	1.695	10550	3940–6407	1461–2377
J224145+122557	2.631	6300	4095–8551	1127–2354
J225409+244523	2.328	1100	3366–6198	1011–1862
J230301-093930	3.454	29700	3837–8352	861–1875
J230444+031145	1.052	4800	3340–6050	1627–2948
J231324+003444	2.083	600	3176–6038	1030–1958
J231543+145606	3.39	9308	3926–7819	894–1781
J233446-090812	3.316	14400	3761–8338	871–1931
J233823+150445	2.418	900	3367–6198	985–1813
J234023-005327	2.085	11400	3048–6305	988–2043
J234352+141014	2.896	16200	3124–6660	801–1709
J234451+343348	3.01	12600	4306–8912	1073–2222
J234531+090906	2.784	11200	3804–6272	1005–1657
J234628+124859	2.573	50000	3022–8934	845–2500
J234632+124540	2.515	15000	3846–6066	1094–1725
J234856-104131	3.172	5600	3102–5980	743–1433
J235010+081255	1.7	1728	3979–6081	1473–2252
J235050+045507	2.593	850	3368–6198	937–1725
J235057-005209	3.025	39989	3897–7494	968–1861
J235129-142756	2.933	13500	3846–6296	977–1600

Table 3 — *Continued*

Object	z_{em}	Total Exp, Time (s)	Wavelength Coverage (Å)	Rest Wavelength Coverage (Å) ^b
J235953-124148	0.868	6000	4317–7455	2311–3990

Note. — ^b Rest wavelength calculated at the Quasar redshift

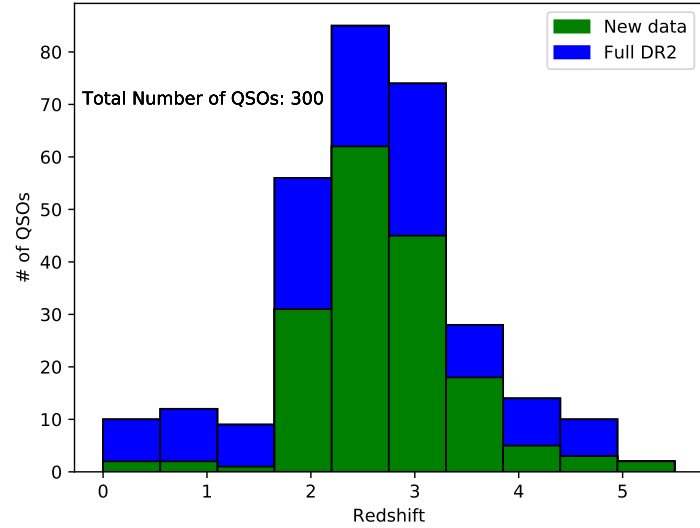


Figure 1. Redshift distribution of KODIAQ DR2 quasars.

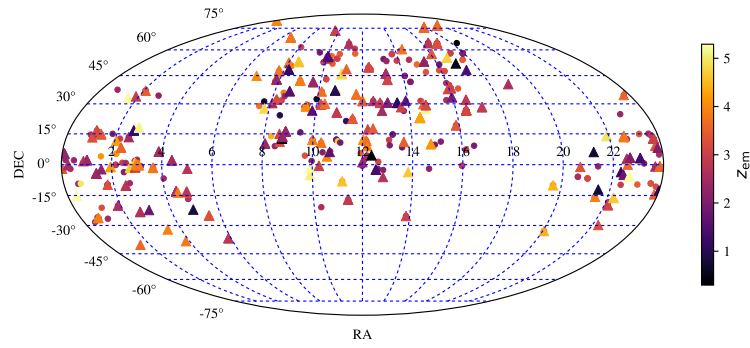


Figure 2. Distribution on the Sky of the KODIAQ DR2 quasars. Triangles correspond to new quasars as presented in Table 2, and circles representing quasars presented in DR1

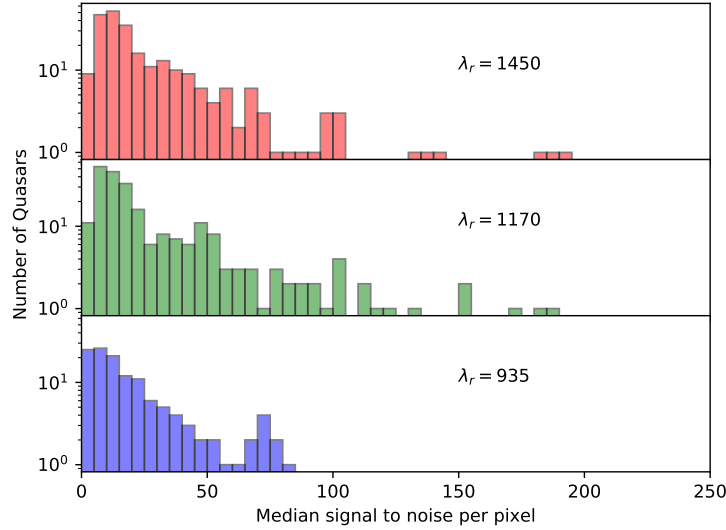


Figure 3. Signal to noise (per pixel) distribution of the co-added spectra in the DR2 sample.

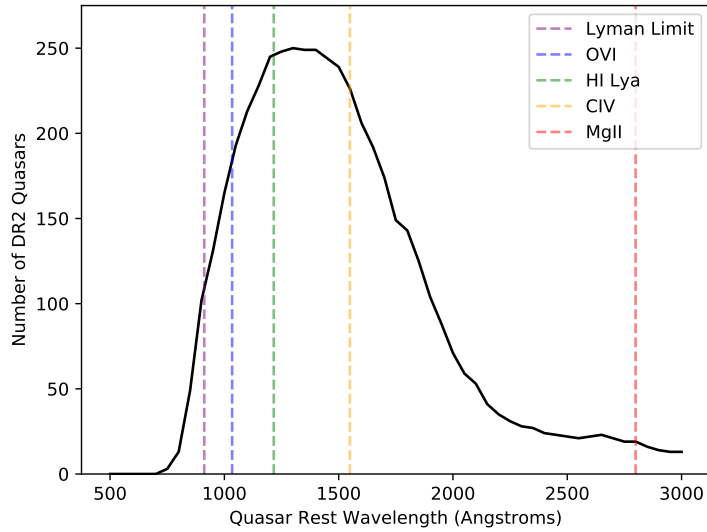


Figure 4. QSO redshift rest wavelength coverage of the DR2 sample. The vertical lines correspond to the rest wavelengths of various commonly studied ions.

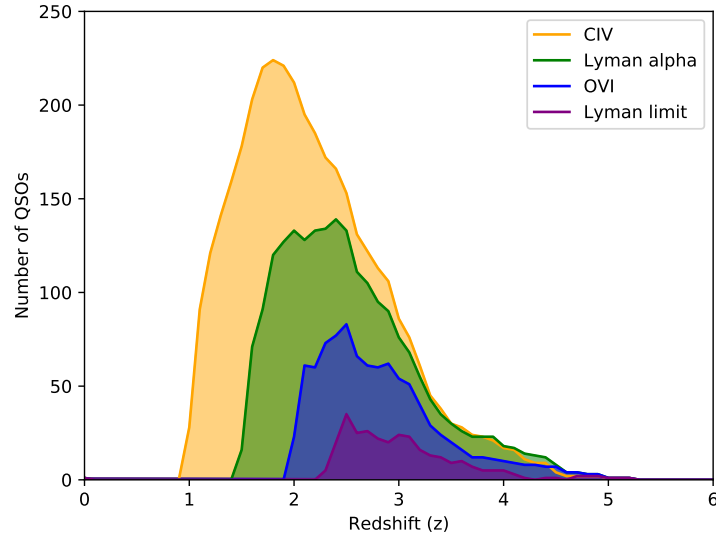


Figure 5. Redshift coverage of intervening absorption from various ions in the DR2 sample.

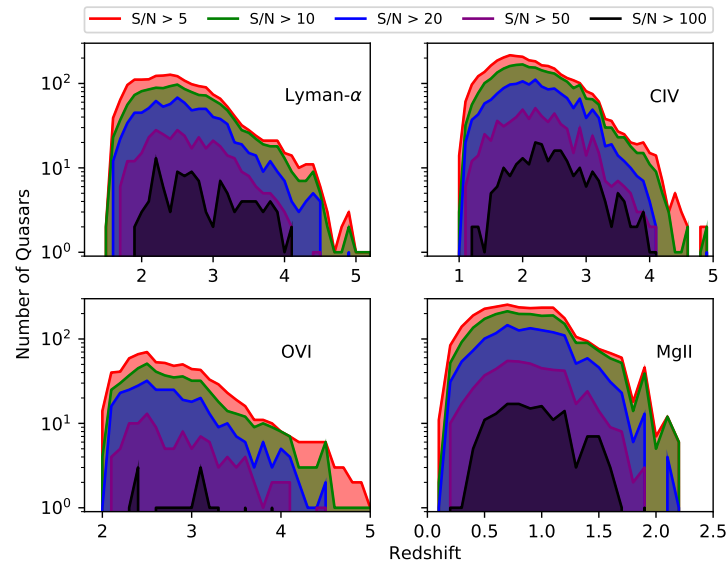


Figure 6. Signal to noise distribution versus redshift for key ions in the DR2 sample.

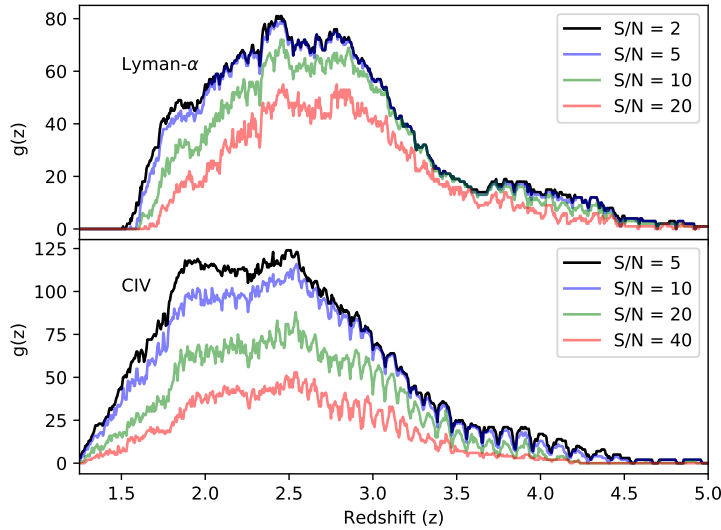


Figure 7. Redshift sensitivity function $g(z)$ for Ly α and C IV in the DR2 as a function of S/N ratio.